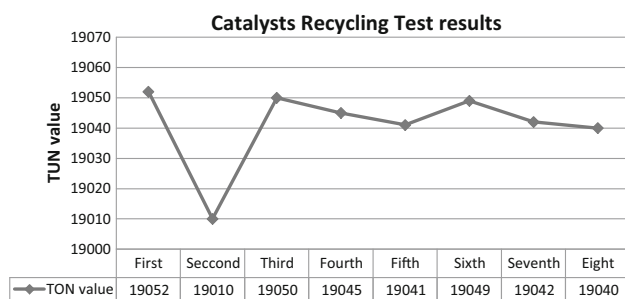CrossMark

Synthesis of Monometallic Ru/TiO$_2$ Catalysts and Selective Hydrogenation of CO$_2$ to Formic Acid in Ionic Liquid

Praveenkumar Upadhyay[1] · Vivek Srivastava[1]

Abstract We successfully synthesized user friendly, stable, agglomeration free monometallic Ru/Ti-x catalyst for ionic liquid mediated CO$_2$ hydrogenation reaction. Two well defined methods (impregnation and deposition–precipitation) were used to prepare 2 wt% Ru/Ti 1–10 catalysts. Advance analytical techniques were applied for the characterization of Ru/Ti-x catalytic systems. A series of functionalized ionic liquids were synthesized and applied as a reaction medium not only for hydrogenation reaction but also as absorbent to solubilize CO$_2$ gas and to anchor the formic acid (hydrogenation product). Such advance application of ionic liquid mediated Ru/Ti-x catalytic system offered the hydrogenation reaction in a more optimized way to achieve maximum selectivity (high TON/TOF value of formic acid) with the added advantage of eight times catalyst recycling.

Graphical Abstract

✉ Vivek Srivastava
vivek.shrivastava@niituniversity.in;
viveksrivastava.job@gmail.com

[1] Basic Sciences: Chemistry, NIIT University, NH-8 Jaipur/
Delhi Highway, Neemrana, Rajasthan 301705, India

Keywords Ru catalyst · MMT clay · Ionic liquid · Carbon sequestration · Formic acid

1 Introduction

The ability to synthesize industrially important chemicals, such as aldehydes, alcohols esters and acids from cheap and renewable chemical source is highly desirable, particularly, if it can be achieved by direct hydrogenation reaction [1–3]. Various transition metal catalysts have been reported in the selective hydrogenation of organic compounds. Transition metal complexes are one of the important hydrogenating catalysts (both homogeneous and heterogeneous) [2, 4, 5]. In various reports Ru, Pd, Pt, Rh, and Zn metal were supported on organic (polymeric and ionic liquids) as well inorganic supports (Silica, clay, zeolite etc.). These modified catalytic systems were applied to different hydrogenation reactions, but unfortunately in most of the reports, these catalytic systems suffer with the tedious catalyst synthesis procedure, high catalyst loading and catalyst leaching during recycling experiments [6–10]. In recent years, nanoparticles have attracted a significant interest due to their potential applications in a variety of organic transformations and hydrogenation is one of them [11–14]. To achieve optimal dispersion and to suppress aggregation of active phases, metal nanoparticles are commonly supported on the surface of solid career [15–18].

The aim of this work was to prepare monometallic Ru/TiO$_2$ catalysts (Ru/Ti-x; x = 1–10 and 6R) with small nanoparticle size in order to maximize the number of low coordination sites available to activate H$_2$ gas, and to evaluate their catalytic performances for the CO$_2$ hydrogenation reaction. In this approach, TiO$_2$ was used as a

support to accommodate Ru metal, as TiO_2 offers wide chemical stability and a non-stoichiometric phase. TiO_2 also counts as a good acidic support and its anatase phase provides a better surface area in order to achieve good catalytic properties [19–23].

The unique physiochemical properties of Ionic liquids such as low melting point, high vapor pressure, good thermal stability, wide temperature range and strong solvating power for various substances (good solubility of heterogeneous/homogeneous catalytic systems) [24–26] makes them promising solvent system over conventional organic solvents. Therefore, ionic liquids were considered as a good alternative for toxic conventional solvent systems. Additionally, functionalized ionic liquids can be achieved by varying cations or anions or by grafting functional groups onto the ions. The functional ionic liquids have been synthesized and applied as catalysts in different organic transformations as well also found applicable in the extraction and absorption of CO_2, SO_2, H_2S and N_2 gases [27–30]. The structural design and synthesis of functional ionic liquids for the specific use or to enhance the efficiency of different processes, is a very interesting and emerging topic in the area of the chemical sciences. Even, to enhance the selectivity of our reaction, we also synthesized and tested a series of functional ionic liquids to absorb CO_2 gas as well to capture partial CO_2 hydrogenated products (formic acid). Use of ionic liquid may also offer easy catalyst isolation and catalyst recycling steps during the reaction [30].

2 Experimental

Reagent Plus® grade chemicals were purchased from Sigma Aldrich and other chemical suppliers. Nuclear Magnetic Resonance (NMR) spectra were recorded on a standard Bruker 300WB spectrometer with an Avance console at 400 and 100 MHz for ¹H NMR. All the hydrogenation reactions were carried out in a 100 mL stainless steel autoclave (Amar Equipment, India). The catalyst material was characterized by TEM (Hitachi S-3700 N) and Energy-dispersive FTIR data for all the samples were studied with Bruker Tensor-27. The morphology of catalysts was investigated by transmission electron microscopy (TEM) using a Philips CM12 instrument. XRD was performed on Philips X-Pert diffractometer. Temperature programmed reduction (H_2-TPR) was used to examine the metal/support interaction and to find out the reduction temperature of catalysts. A H_2-TPR experiment was carried out in a Micrometrics 2920 Auto-Chem II chemisorption analyzer, equipped with thermal conductivity detector (TCD). 0.2 g of catalyst was placed in sample holder and TPR was performed in the temperature range of 0–400 °C with a heating rate of 10 °C/min. The H_2 consumption was monitored by a TCD. BET surface area, pore size, and pore volume measurements of the catalysts were determined from a physical adsorption of N_2 using liquid nitrogen by an ASAP2420 Micromeritics adsorption analyzer (Micromeritics Instruments Inc.). All the samples were degaussed at the 250 °C for 2 h prior to the measurements to remove the adsorbed moisture from catalysts surface and pores. The surface area and pore size distribution (PSD) were calculated from the BET and BJH equations, respectively, by the instrument software.

3 Synthesis of Catalyst

Two commercially available titania (Degussa P-25 and CristalACTiV™ DT-51), were used as support for Ru metal. TiO_2, denoted by TiO_2 (Synth), was synthesized in lab followed by sol gel method using titanium isopropoxide as precursor and PEG-400 as templating agent. The reaction mixtures obtained from these two solutions were maintained under stirring at 40 °C for 1 h and thereafter further treated in a closed Teflon vessel at 60 °C for 7 h. Finally, a white solid was recovered by filtration and further dried in vacuum oven under reduced pressure at 50 °C for next 5 h.

Two different approaches (impregnation or deposition–precipitation method) were used for the synthesis of monometallic 2.0 wt% Ru/Ti-x catalysts.

In impregnation method (IMPR), we used four different types Ru metal precursors (0.21 g) such as $[Ru(NH_3)_6]Cl_3$, $Ru(NO)(NO_3)_3$, $RuCl_3 \cdot 3H_2O$ and $Ru(acac)_3$. The impregnation method was started by preparing an aqueous solution of Ru metal precursor salt (10 %, 100 mL) with defined pH value (1 or 11).The pH of the aqueous metal salt solution was controlled by the addition of ammonium hydroxide (17 wt%) or chlrohydric acid (32 wt%) respectively. The defined pH value helps metal ions to interaction with support during the impregnation method. All types of available titania (10 g) were used in the impregnation method for preparing Ru/Ti-x catalysts. After successful completion of all the impregnation steps, the solvent was evaporated in lyophilizer and the catalyst was further dried under vacuum at 100 °C for 8 h. The calcination of perfectly dried impregnated Ru/Ti-x catalysts were carried out under artificial air flow (90 % N_2 + 10 % O_2, 2 L/h) with temperature range 350–400 °C for 5 h. Catalyst reduction was carried out under hydrogen pressure (4 bar) in high pressure autoclave for 2 h at 30 °C before using the catalyst for hydrogenation reaction.

The deposition–precipitation method (DP), was carried out using by making a slurry of Ru metal precursor salt

(0.25 g, 10 % aqueous solution in 100 mL water) to the suspension of titania (10 g) in distilled water (50 mL). Again pH was adjusted at 11 by adding aqueous solution of NaOH (10 wt%). The resulting suspension was refluxed for 1 h. After cooling the reaction mass, solid material was filtered and dried in a vacuum oven for 5 h at 100 °C. Later, catalysts were hydrogenated under hydrogen atmosphere (4 bar) in a high pressure autoclave for next 12 h at 30 °C before using them as catalyst.

The amount of ruthenium metal (wt%) in Ru/Ti-x catalysts were calculated (before and after the reduction of Ru/Ti-x) using inductively coupled plasma atomic emission spectrometer (ICP-AES, ARCOS from M/s. Spectro, Germany) [31, 32]. 0.1 g of sample was digested in a minimum amount of conc. HNO_3 with heating, and volume made up to 10 mL. The obtained results confirmed the presence of Ru (2 wt%) in every Ru/Ti-x catalyst, only in case of Ru Ti-10 the Ru loading was 1.8 wt%. All the Ru Ti catalysts were obtained with negligible product loss after all the work-up process.

4 Synthesis of Ionic Liquids

Ionic liquids like 1-(*N*,*N*-dimethylaminoethyl) 2,3-dimethy limidazolium trifluoromethanesulfonate ([mammim][TfO]), and 1,3-*di*(*N*,*N*-dimethylaminoethyl)-2-methylimidazolium *bis* (trifluoromethylsulfonyl) imide ([DAMI][NTf₂])were synthesized as per the reported procedures [31, 32] while ionic liquids such as 1-(*N*,*N*-dimethylaminoethyl) 2,3-dimethylimidazolium *bis* (trifluoromethylsulfonyl) imide ([mammim][NTf₂]), 1-(*N*,*N*-dimethylaminoethyl)-2,3-dimethylimidazolium nonafluorobutanesulfonate ([mammim [CF₃CF₂CF₂CF₂SO₃]), 1-(*N*,*N*-dimethylaminoethyl)-2,3-dimethylimidazolium trifluoromethanesulfonate ([mammim [BF₄]), 1,3-*di*(*N*,*N*-dimethylaminoethyl)-2-methylimidazolium trifluoromethanesulfonate ([DAMI][TfO]), 1,3-*di*(*N*,*N*-dimethylaminoethyl)-2-methylimidazolium nonafluorobutanesulfonate ([DAMI][CF₃CF₂CF₂CF₂SO₃]) and 1,3-*di*(*N*,*N*-dimethylaminoethyl)-2-methylimidazolium tetrafluoroborate ([DAMI][BF₄]) were synthesized. All the analytical data with respect to synthesized ionic liquids were obtained in good agreement with their reported analytical data [31–33].

4.1 Synthesis of Monoamine/Diamine Functionalized Ionic Liquids

The 250 mL, single neck round bottom flask was charged with methanol (100 mL), NaOH (1.1 equiv) and 1-(*N*,*N*-dimethylaminoethyl)-2,3-dimethylimidazolium bromide hydrobromide or,3-di(*N*,*N*-dimethylaminoethyl)-2-methylimidazolium bromide dihydrobromide (1 equiv) [30–32]. The total reaction mixture was allowed to stir for 1 h at room

temperature (25–30 °C). 50 % aqueous solution of sodium tetrafluoroborate or lithium *bis* (trifluoromethylsulfonyl) imide or Lithium nonafluorobutanesulfonate (1.1 equiv) was then added and the mixture stirred for 2 h at room temperature. The water was evaporated under reduced pressure then dichloromethane (100 mL) was added, and the mixture was stirred for 1 h. The solid (NaBr) was isolated by simple filtration as a side product, dichloromethane was removed from the filtrate under reduced pressure on the water bath, and the resulting derided ionic liquid (Table 4) was dried at 50 °C for 2 h under high vacuum. The concentration of water in all ionic liquids was calculated by Karl–Fischer analysis and it was found less than 0.01 wt%.

The structure of the all the synthesized mono and diamino functionalized ionic liquids was confirmed by ^{1}H NMR and HRMS.

4.1.1 [mammim][NTf₂]

^{1}H NMR (400 MHz, CDCl₃): δ 2.17 (s, 6H), δ 2.52 (s, 3H), δ 2.71 (t, 2H), δ 3.59 (s, 3H), δ 4.17 (t, 2H), δ 7.25 (d, 1H), δ 7.28 (d, 1H). Positive ion HRMS (EI) m/z found: 426.2256 (calculated for $C_{17}H_{37}N_4O_4S_2$, M$^+$ requires: 426.2289).

4.1.2 [mammim][CF₃CF₂CF₂CF₂SO₃]

^{1}H NMR (400 MHz, MeOD): δ 2.15 (s, 6H), δ 2.55 (s, 3H), δ 2.31 (t, 2H), δ 3.62 (s, 3H), δ 4.19 (t, 2H), δ 7.23 (d, 1H), δ 7.30 (d, 1H). Positive ion HRMS (EI) m/z found: 468.1003 (calculated for $C_{13}H_{19}F_9N_3O_3S$, M$^+$ requires: 468.1002).

4.1.3 [mammim][BF₄]

^{1}H NMR (400 MHz, CDCl₃): δ 2.11 (s, 6H), δ 2.45 (s, 3H), δ 2.37 (t,2H), δ 3.65 (s, 3H), δ 4.22 (t, 2H), δ 7.28 (d, 1H), δ 7.35 (d, 1H). Positive ion HRMS (EI) m/z found: 265.1504 (calculated for $C_9H_{19}BF_4N_3$, M$^+$ requires: 256.1608).

4.1.4 [DAMI][CF₃CF₂CF₂CF₂SO₃]

^{1}H NMR (400 MHz, MeOD): d = 2.58 (s, 12H), 2.82 (s, 3H), 2.89 (t, 4H), 4.49 (s, 4H), 7.71 ppm (d, 2H). Positive ion HRMS (EI) m/z found: 313.1663 (calculated for $C_{12}H_{26}BF_4N_4$, M$^+$ requires: 313.2181).

4.1.5 [DAMI] [BF₄]

^{1}H NMR (400 MHz, CDCl₃): d = 2.48 (s, 12H), 2.79 (s, 3H), 2.85 (t, 4H), 4.42 (s, 4H), 7.70 ppm (d, 2H). Positive ion HRMS (EI) m/z found: 525.1542 (calculated for $C_{16}H_{26}F_9O_3S$, M$^+$ requires: 525.1580).

4.2 CO$_2$ loading on Ionic liquids [29, 30, 34]

In a typical procedure, the CO$_2$ capture was carried out in high pressure autoclave (100 mL). The absorbents were charged into the reactor at room temperature. Then, the air in the flask was replaced by passing CO$_2$. The absorption was conducted at 80 °C with a 4 bar CO$_2$ gas for 1 h. The amount of CO$_2$ absorbed was determined by calculating the weight of the reaction mixture with an analytical balance. Data points were taken with an accuracy of ±0.0001 g every five minutes. At 80 °C slight while at 100 °C complete desorption of CO$_2$ was recorded.

5 CO$_2$ Hydrogenation Reaction

The 100 mL autoclave was charged with solvent and catalyst (pre reduced) as per Table 5. Then the oxygen of reaction vessel was replaced by CO$_2$/H$_2$ gas. Reaction mass was allowed to stir as per Table 5. Later, the reaction vessel was cooled (2–5 °C) with the help of cold water supply. A small amount of crude reaction mass was used for ^{1}HNMR analysis. Water was evaporated from the reaction mass at 110 °C under reduced pressure, then only formic acid was isolated from the reaction mass with the help of nitrogen gas flow at 125–130 °C, passing through the water trap, in order to capture formic acid with minimum loss in recovery process. Acid

base titration was used to calculate the amount formic acid in water trap. The results obtained from ^{1}HNMR analysis as well as from titration method were found in full agreement.

The recovered catalyst and ionic liquid were reused directly in subsequent experiments, where, the [DAMI][CF$_3$CF$_2$CF$_2$CF$_2$SO$_3$] ionic liquid immobilized Ru/Ti-6 catalyst was allowed to stir under argon atmosphere (2 bars) for 1 h at room temperature. Later, argon was replaced by hydrogen gas and reaction mass was stirred under hydrogen atmosphere (4 bars) for 2 h at 30 °C and then all the steps were completed as per above mentioned CO$_2$ hydrogenation reaction protocol.

6 Result and Discussion

Initially, we characterized all the TiO$_2$ materials, which were used to support monometallic Ru species (Table 1). The surface area, pore volume and pore diameter were calculated using N$_2$ sorption method.

Table 2, summarizes the physiochemical properties of all the monometallic Ru/Ti-x catalysts prepared by impregnation method (IPMR) or by deposition–precipitation method (DP). Ru/Ti-x catalysts were synthesized via the impregnation method, several parameters were modulated in order to obtain the optimized dispersion of Ru metal over TiO$_2$ support. The dispersion analysis of Ru/

Table 1 Types of TiO$_2$ supports and their physiochemical properties

TiO$_2$ types	Surface area (m^2/g)	Pore volume	Pore diameter	Average crystal size (nm)
P-25	50	0.11	13.2	18 (anatase)
				35 (rutile)
DT-51	85	0.28	11.1	17 (anatase)
TiO$_2$ (synth)	190	0.31	6.1	6 (anatase)

Table 2 Types of synthesized Ru/TiO$_2$catalysts and their characterization

Catalysts	Metal precursor salt	Precipitation method	pH	Calcination temperature (°C)	Reduction temperature (°C)	Type of TiO$_2$	Ru metal DP	Particle Size or Ru (nm)		BET surface area
								H$_2$-Value	TEM data	
Ru/Ti-1	[Ru(NH$_3$)$_6$]Cl$_3$	IPMR	11	250	250	P-25	12	7.5	7.5	25.1
Ru/Ti-2	Ru(NO)(NO$_3$)$_3$	IPMR	11	250	250	P-25	13	8.1	8.8	27.1
Ru/Ti-3	Ru Cl$_3$·3H$_2$O	IPMR	11	250	250	P-25	11	9.5	9.8	23.5
Ru/Ti-4	Ru(acac)$_3$	IPMR	11	250	250	P-25	17	9.1	9.6	29.0
Ru/Ti-5	Ru Cl$_3$·3H$_2$O	IPMR	11	300	250	P-25	25	6.8	7.1	39.0
Ru/Ti-6	Ru Cl$_3$·3H$_2$O	IPMR	11	250	300	P-25	30	6.1	6.8	41.2
Ru/Ti-7	Ru Cl$_3$·3H$_2$O	IPMR	11	250	300	P-25	23	6.9	7.3	37.7
Ru/Ti-8	Ru Cl$_3$·3H$_2$O	IPMR	5	250	300	P-25	8	6.0	6.7	10.8
Ru/Ti-9	Ru Cl$_3$·3H$_2$O	IPMR	11	300	250	Synth	24	8	8.9	160
Ru/Ti-10	Ru Cl$_3$·3H$_2$O	DP	11	300	250	DT-51	14	11.6	12.7	72
Ru/Ti-6R	Ru Cl$_3$·3H$_2$O	IPMR	11	250	300		23	7.1	7.8	31.2

TiO_2 catalysts was carried out by H_2 chemisorption method. As per Table 2, we used four different types of Ru metal salt precursors either to impregnate or to deposit it on TiO_2 support. Among all the results, we obtained well dispersed and small particle size of Ru metal in Ru/Ti-6 catalyst, where the $RuCl_3$ was impregnated on TiO_2 (P-25) at pH 11. Surprisingly, at low pH, while preparing Ru/Ti-8 catalyst, the dispersion value was found very low. The best dispersion of Ru metal was obtained in, Ru/Ti-4 to Ru/Ti-7 and RuTi-9 catalysts. However, the considering the particle size of Ru, we found the smallest Ru particles in Ru/Ti-6 catalyst and average Ru metal dispersion. It is important to notify that we successfully synthesized highly dispersed, agglomeration free and stable TiO_2 supported Ru catalyst to hydrogenate CO_2 gas. The BET surface area for different Ru/Ti-x catalysts using N_2 physisorption methods and all the results were summarized in Table 3. The BET surface area of pure TiO_2 supports was decreased with increasing the Ru metal loading [30].

The H_2-TPR method was used to understand the reduction behavior of Ru metal as well as its interaction with TiO_2 support (Fig. 1; Table 3). As per Table 3, catalysts showed the basic reduction peak in the temperature range 80–115 °C for Ru^{+3}/Ru^o. In some of the catalysts, we observed the second peak in the temperature rage 150–180 °C, which indicated the reduction of oxychlorides during catalyst synthesis. High temperature broad peak appears in the region of 350–400 °C, for Ru/Ti-1/2/9/10 catalyst which confirms the presence of some oxidized Ru metal and offered strong metal support interaction. Hydrogen consumption value also indicates the presence of Ru loading and it was found maximum in case of Ru/Ti-6 catalyst.

The size and the morphology the synthesized Ru/Ti-x catalysts were also investigated using TEM analysis (Fig. 2a–d). The TEM image of Ru/Ti-6/9/10, were given in Fig. 1. The particle size of catalysts lies between 6 and 12 (± 0.5) nm and it was found in good agreement with their corresponding XRD data (Fig. 3). In catalyst Ru/Ti-6, the Ru metal appears in dark spots and uniformly distributed over TiO_2. A sign of agglomeration was found in Ru-Ti-10 catalyst and it was confirmed by some dark patches as well as the formation of metallic culture with non-uniform distribution in its TEM image (Fig. 2).

The crystalline natures of the materials were investigated using powder X-ray analysis (Fig. 3). The XRD data for pure and Ru-TiO_2 catalysts were arranged in Fig. 1. It is worth noted here that some of the XRD data did not show any XRD peak ascribed to the presence of deposited metal which confirms the ultrafine dispersion as well as formation of very small cultures of Ru particles over TiO_2 support. It was also analyzed in XRD study that the rutile/ anatase structure as well as the morphology of TiO_2 remains same after supporting the Ru metal onto it.

6.1 Hydrogenation Reaction of CO_2 to Formic Acid

Anxieties over carbon dioxide levels in our atmosphere have reached ca. 400 p.p.m. are leading to scientific/technological efforts to reduce CO_2 emissions. Converting CO_2 gas into useful feedstock/platform chemicals and fuels offers a beneficial way to not only lower the CO_2 level from the atmosphere, but also to synthesize chemicals using cheap source [35–39]. In recent years, several reactions have been studied and commercialized for the same reaction [37, 38]. In one of the previous reports, we also

Table 3 TPR study on the reduction behavior of Ru/TiO_2 catalysts

Support/Catalysts	T_1^{max} (°C)	H_2 uptake (g/mol)	T_2^{max} (°C)	H_2 uptake (g/mol)	T_3^{max} (°C)	H_2 uptake (g/mol)	Total H_2 uptake (mol/g)
P-25	48	0.0	–	–	–	–	0.0
DT-51	67	0.0	–	–	–	–	0.0
TiO_2 (synth)	87	0.0	–	–	–	–	0.0
Ru/Ti-1	75	30	160	45	380	112	187
Ru/Ti-2	88	57	–		385	30	87
Ru/Ti-3	69	46	–		–	–	46
Ru/Ti-4	97	81	169	80	–	–	161
Ru/Ti-5	101	138	–	–	–	–	138
Ru/Ti-6	113	275	–	–	–	–	275
Ru/Ti-7	109	113	–	–	–	–	113
Ru/Ti-8	98	92	–	–	–	–	92
Ru/Ti-9	102	60	178	45	395	40	145
Ru/Ti-10	104	120	180	50	390	30	180
Ru/Ti-6-R	112	52	185	32	–	–	84

Fig. 1 TRP study of Ru/TiO₂ catalysts

(a) Ru/Ti-6

(b) Ru/Ti-9

(c) Ru/Ti-10

(d) Ru/Ti-6 (after catalysis)
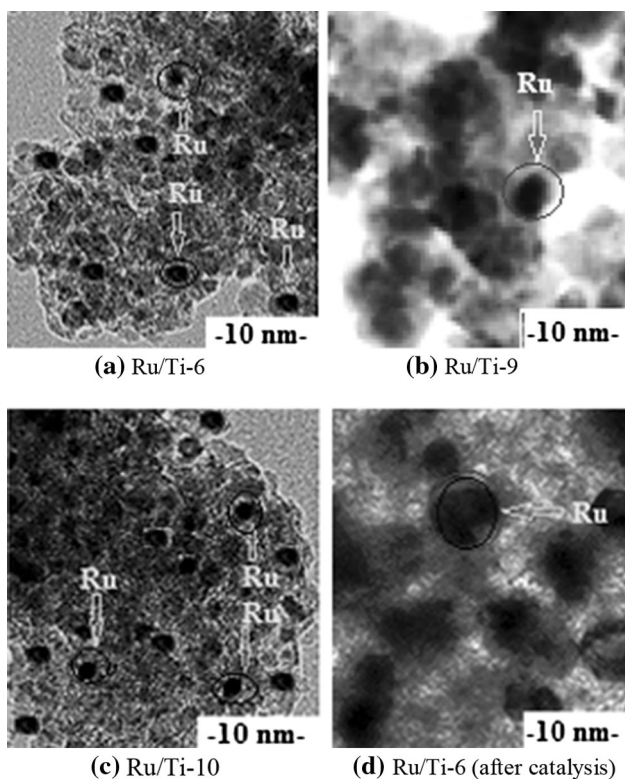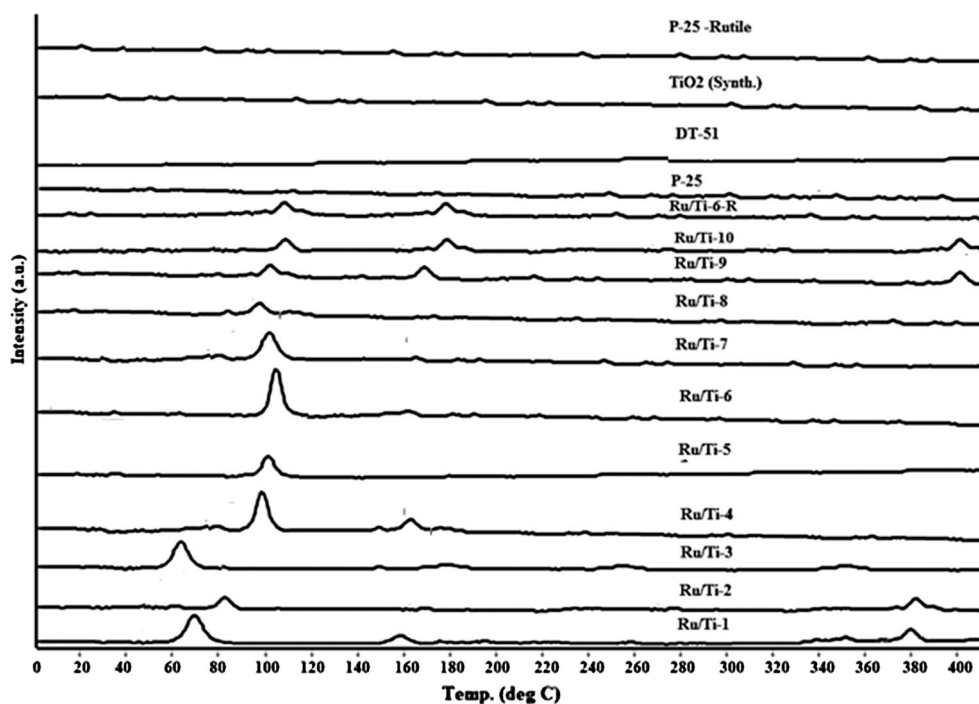
Fig. 2 TEM analysis of Ru/TiO₂ catalysts

developed some modified Ru catalysts to get formic acid followed by selective hydrogenation CO₂. In our previous study, we found two most important driving forces (1. supporting the Ru metal over MMT clay or immobilizing Ru nanoparticles in ionic liquid; 2. application of ionic liquid as a reaction medium) to achieve the formic acid in good TON/TOF value with the added advantages of low catalyst loading and catalyst recycling [31, 32].

Recently, the applications of ionic liquids were also exploited to carbon capture and it's separation process. Various research groups reported their work to study the CO₂ solubility in ionic liquids [31, 32]. In the continuation of our work, we synthesized a series of imodazolium based functionalized ionic liquids, which can not only trap the formic acid as well as also provided maximum solubility to CO₂ gas. In order to improve the CO₂ solubility in ionic liquids, two approaches have been applied, First, modification in the imidazolium cation using addition of branched chains or some polar groups, such expansion in the cations of ionic liquid increases the free volume to accommodate CO₂ gas. Second, addition of functional CO₂-philic groups or anions in ionic liquid too stabilizes the surrounding CO₂ [27–30]. In addition, the physiochemical properties of anions in ionic liquids play a significant role in the solubility of CO₂ gas than the cations [29, 30]. Ionic liquid carrying highly fluorinated anions, were recorded to have the highest CO₂ solubility among the ionic liquids with the same cations [29]. Apart from such advantages, C-F bond of anions increases the rigidity and decreases the polarity of ionic liquid [30]. Such change in the properties of ionic liquid, not only leads to higher gas solubility in highly fluorinated ionic liquids, but also makes easy regeneration of the ionic liquid.

We synthesized a series of ionic liquids having single or double tertiary amino group on the cations, not only to
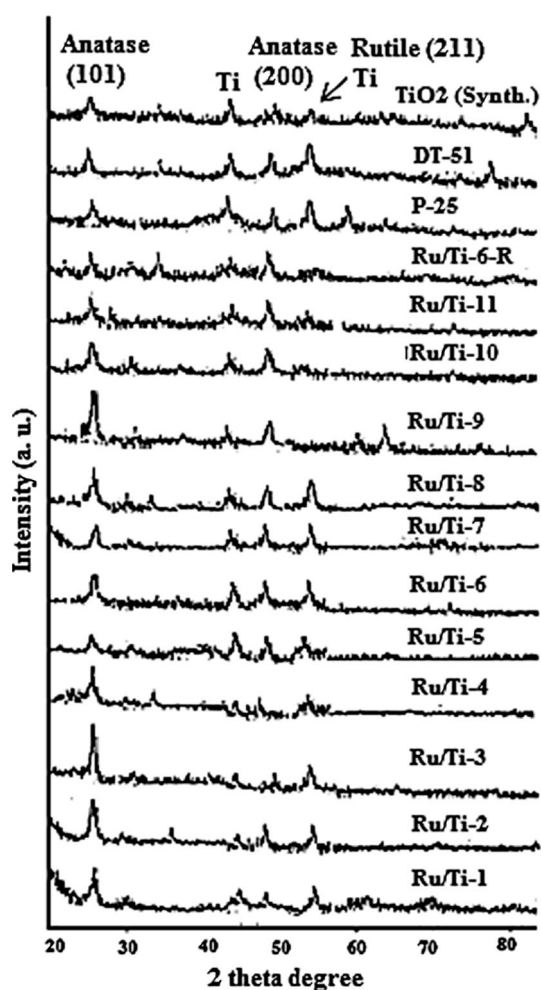
Fig. 3 XRD data of Ru/TiO$_2$ catalysts

promote the hydrogenation of CO_2, but also to trap the formic acid (easy recovery of product) after the reaction. The $-CH_2CH_2-$ chain of $-CH_2CH_2NH_2$ is also expected to provide free volume for enhanced CO_2 occupation. It is important to notify here, that the nature of anions in ionic liquid plays an important role in the solubility of CO_2 over the cationic part of ionic liquid. In addition, we also decided to incorporate fluorinated as well as sulfated anions to ionic liquids, as it is well reported in literature that they offers highest CO_2 solubility among the ionic liquids with the same cations [31, 32].

In the initial part of our study, we tested the absorption performance of the following functionalized ionic liquids; [mammim][NTf$_2$], [mammim][TfO], [mammim][CF$_3$CF$_2$CF$_2$CF$_2$SO$_3$], [mammim][BF$_4$], [DAMI][TfO], [DAMI][NTf$_2$], [DAMI][CF$_3$CF$_2$CF$_2$CF$_2$SO$_3$] and [DAMI][BF$_4$] at 50 °C for 1 h in pressure autoclave with 20 bar CO_2 gas (Table 4). Among, all the ionic liquid, we obtained the maximum solubility of CO_2 in [DAMI][CF$_3$CF$_2$CF$_2$CF$_2$SO$_3$]) ionic liquid. It was clearly found that the CO_2 accommodation was increased while increasing the alkyl side chain on the cationic part of the ionic liquid and we got the maximum loading of CO_2. The CO_2-philic nature of sulfated and fluorinated anions of ionic liquids, also enhances the solubility CO_2 gas.

After getting the best result with [DAMI][CF$_3$CF$_2$CF$_2$CF$_2$SO$_3$] functionalized ionic liquid in terms of CO_2 loading, we optimized our monometallic Ru/TiO$_2$ catalysts to achieve selective hydrogenation of CO_2 to formic acid in terms of high TON/TOF value (Table 5, entry 1–36). Hydrogenation of CO_2 was carried out using H$_2$ gas in the presence of Ru/Ti-6 catalysts in [DAMI] [CF$_3$CF$_2$CF$_2$

Table 4 Absorption study of CO_2 over ionic liquids

Ionic liquid	CO_2 pressure (bar)	Temperature (°C)	Time (h)	CO_2 loading[a]
[mammim][NTf$_2$]	20	80	1	25
[mammim][TfO]	20	80	1	41
[mammim][CF$_3$CF$_2$CF$_2$CF$_2$SO$_3$]	20	80	1	47
[mammim][BF$_4$]	20	80	1	13
[DAMI][TfO]	20	80	1	51
[DAMI][NTf$_2$]	20	80	1	48
[DAMI][CF$_3$CF$_2$CF$_2$CF$_2$SO$_3$]	20	80	1	68
[DAMI][BF$_4$)	20	80	1	21
[DAMI][CF$_3$CF$_2$CF$_2$CF$_2$SO$_3$]	10	80	1	31
[DAMI][CF$_3$CF$_2$CF$_2$CF$_2$SO$_3$]	25	80	1	70
[DAMI][CF$_3$CF$_2$CF$_2$CF$_2$SO$_3$]	20	50	1	65
[DAMI][CF$_3$CF$_2$CF$_2$CF$_2$SO$_3$]	20	100	1	35
[DAMI][CF$_3$CF$_2$CF$_2$CF$_2$SO$_3$]	20	80	3	69
[DAMI][CF$_3$CF$_2$CF$_2$CF$_2$SO$_3$]	20	80	0.5	23

[a] Mole of CO_2 captured per mol of ionic liquid

Table 5 Hydrogenation of CO$_2$ to formic acid using ionic liquid immobilized Ru/TiO$_2$

Entry[a]	Catalytic system	Solvent system	P (H$_2$) (P_{total}) (MPa)[b]	Tem. (°C)	Time (h)	TON[c]	TOF[d]
1	Ru/Ti-6	[DAMI][CF$_3$CF$_2$CF$_2$CF$_2$SO$_3$]	30 (60)	80	5	16,801	3360
2	Ru/Ti-6	[DAMI][CF$_3$CF$_2$CF$_2$CF$_2$SO$_3$]	30 (60)	50	5	9856	971
3	Ru/Ti-6	[DAMI][CF$_3$CF$_2$CF$_2$CF$_2$SO$_3$]	30 (60)	100	5	9521	1904
4	Ru/Ti-6	[DAMI][CF$_3$CF$_2$CF$_2$CF$_2$SO$_3$]	30 (60)	120	5	6645	1329
5	Ru/Ti-6	[DAMI][CF$_3$CF$_2$CF$_2$CF$_2$SO$_3$]	30 (60)	80	7	16,899	2414
6	Ru/Ti-6	[DAMI][CF$_3$CF$_2$CF$_2$CF$_2$SO$_3$]	30 (60)	80	2	10,614	5307
7	Ru/Ti-6	[DAMI][CF$_3$CF$_2$CF$_2$CF$_2$SO$_3$]	20 (40)	80	5	10,651	2130
8	Ru/Ti-6	[DAMI][CF$_3$CF$_2$CF$_2$CF$_2$SO$_3$]	50 (100)	80	5	11,232	2246
9	Ru/Ti-6	[DAMI][CF$_3$CF$_2$CF$_2$CF$_2$SO$_3$] + H$_2$O (1 mL)	30 (60)	80	5	17,541	3508
10	Ru/Ti-6	[DAMI][CF$_3$CF$_2$CF$_2$CF$_2$SO$_3$] + H$_2$O (2 mL)	30 (60)	80	5	19,052	3810
11	Ru/Ti-6	[DAMI][CF$_3$CF$_2$CF$_2$CF$_2$SO$_3$] + H$_2$O (3 mL)	30 (60)	80	5	19,050	3813
12	Ru/Ti-6	[DAMI][CF$_3$CF$_2$CF$_2$CF$_2$SO$_3$] (0.05 g) + H$_2$O (2 mL)	30 (60)	80	5	8712	1742
13	Ru/Ti-6	[DAMI][CF$_3$CF$_2$CF$_2$CF$_2$SO$_3$] (0.150 g) + H$_2$O (2 mL)	30 (60)	80	5	16,901	3380
14	Ru/Ti-6	H$_2$O (2 mL)	30 (60)	80	5	421	84
15	Ru/Ti-6	[DAMI][CF$_3$CF$_2$CF$_2$CF$_2$SO$_3$] + H$_2$O (2 mL)	30 (60)	80	5	12,685	2537
16	Ru/Ti-6 (0.100 g)	[DAMI][CF$_3$CF$_2$CF$_2$CF$_2$SO$_3$] + H$_2$O (2 mL)	30 (60)	80	5	16,923	3385
17	Ru/Ti 6 (0.02 g)	[DAMI][CF$_3$CF$_2$CF$_2$CF$_2$SO$_3$] + H$_2$O (2 mL)	30 (60)	80	5	10,431	2086
18	Ru/Ti-6	[DAMI][CF$_3$CF$_2$CF$_2$CF$_2$SO$_3$] + H$_2$O (2 mL) + PPh$_3$ (0.01 mol)	30 (60)	80	5	19,055	3811
19	Ru/Ti-6	[mammim][NTf$_2$]	30 (60)	80	5	10,527	2105
20	Ru/Ti-6	[mammim][TfO]	30 (60)	80	5	12,679	2536
21	Ru/Ti-6	[mammim][CF$_3$CF$_2$CF$_2$CF$_2$SO$_3$]	30 (60)	80	5	12,998	2600
22	Ru/Ti-6	[mammim][BF$_4$]	30 (60)	80	5	9891	1978
23	Ru/Ti-6	[DAMI][TfO]	30 (60)	80	5	13,427	2685
24	Ru/Ti-6	[DAMI][NTf$_2$]	30 (60)	80	5	11,827	2365
25	Ru/Ti-6	[DAMI][BF$_4$)	30 (60)	80	5	10,964	2193
26	Ru/Ti-1	[DAMI][CF$_3$CF$_2$CF$_2$CF$_2$SO$_3$] + H$_2$O (2 mL)	30 (60)	80	5	8956	1791
27	Ru/Ti-2	[DAMI][CF$_3$CF$_2$CF$_2$CF$_2$SO$_3$] + H$_2$O (2 mL)	30 (60)	80	5	9861	1972
28	Ru/Ti-3	[DAMI][CF$_3$CF$_2$CF$_2$CF$_2$SO$_3$] + H$_2$O (2 mL)	30 (60)	80	5	8393	1679
29	Ru/Ti-4	[DAMI][CF$_3$CF$_2$CF$_2$CF$_2$SO$_3$] + H$_2$O (2 mL)	30 (60)	80	5	10,124	2025
30	Ru/Ti-5	[DAMI][CF$_3$CF$_2$CF$_2$CF$_2$SO$_3$] + H$_2$O (2 mL)	30 (60)	80	5	11,671	2334
31	Ru/Ti-7	[DAMI][CF$_3$CF$_2$CF$_2$CF$_2$SO$_3$] + H$_2$O (2 mL)	30 (60)	80	5	12,623	2525
32	Ru/Ti-8	[DAMI][CF$_3$CF$_2$CF$_2$CF$_2$SO$_3$] + H$_2$O (2 mL)	30 (60)	80	5	11,971	2394
33	Ru/Ti-9	[DAMI][CF$_3$CF$_2$CF$_2$CF$_2$SO$_3$] + H$_2$O (2 mL)	30 (60)	80	5	11,972	2394
34	Ru/Ti-10	[DAMI][CF$_3$CF$_2$CF$_2$CF$_2$SO$_3$] + H$_2$O (2 mL)	30 (60)	80	5	7231	1446
35	RuCl$_3$·3H$_2$O	[DAMI][CF$_3$CF$_2$CF$_2$CF$_2$SO$_3$] + H$_2$O (2 mL)	30 (60)	80	5	7827	1565
36	–	H$_2$O (2 mL)	30 (60)	80	5	nd	nd

[a] Reaction conditions: 0.05 g of catalyst and 0.100 g ionic liquid

[b] The total pressure of the system is indicated in parentheses

[c] Turn over number = n (formic acid) n (Ru)$^{-1}$ in one reaction cycle

[d] Turnover frequency = n (formic acid) n (Ru)$^{-1}$h^{-1}; 4. RuCl$_3$·xH$_2$O (50 % Ru metal)

CF$_2$SO$_3$] ionic liquid medium at 80 °C in the high pressure reactor. After 2 h, formic acid was isolated from the reaction mass followed by the nitrogen flow at 125–130 °C. The results obtained during reaction optimization with respect to TON/TOF value of formic acid were summarized in Table 5, entry 1–36. Acid–base titration using phenolphthalein indicator and ^{1}H NMR analysis

was used to calculate the quantity of formic acid formed after the hydrogenation reaction. ^{1}H NMR analysis also confirmed no decomposition of formic acid as well as an ionic liquid during the experimental condition.

While optimizing the reaction temperature for hydrogenation reaction, we obtained less TON value of formic acid while lowering as well as increasing the temperature
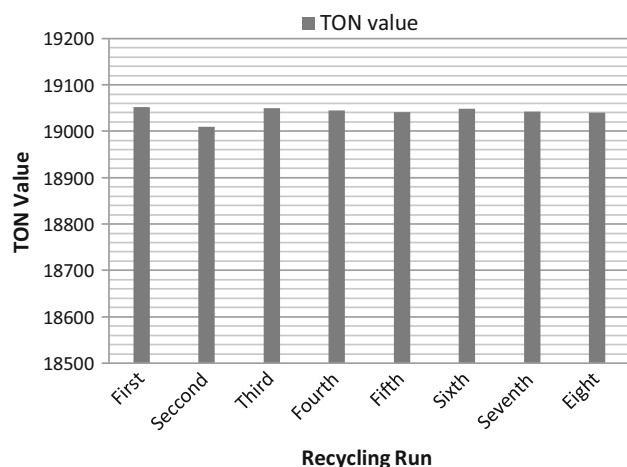
Fig. 4 Catalysts recycling experiment test results

(Table 5, entry 2–4). Increase in temperature may cause separation of absorbed CO_2 from the ionic liquid framework while at low temperature (50 °C) catalyst was not found active enough to accelerate CO_2 hydrogenation reaction. The kinetic effect of water was also studied to enhance the CO_2 hydrogenation reaction rate.

The reaction kinetics of hydrogenation reaction was improved with 2 mL of water and we obtained the formic acid in high TON value (Table 5, entry 9–11). Such improvement mainly happened because the CO_2 gas was reacted with water and it offered bicarbonates which may act as a perfect substrate for the hydrogenation reaction. Quantities of ionic liquid as Ru/Ti-6 catalyst were also optimized (Table 5, entry 12–17). Suprisingly, a slight increase in the TON value of formic acid was found, in the presence of triphenylphosphine (PPh_3) (Table 5, entry 18).

After getting an optimized reaction condition, we also screened our other developed catalysts as well as ionic liquids (Table 5, entry 19–23). The low TON value of formic acid were obtained with Ru/Ti-10 catalysts as some amount of Ru metal agglomeration was observed in its TEM analysis (agglomeration confirms the deactivation of catalyst).

The results obtained in the Table 4, clearly reflected that one mole diamine functionalized ionic liquid, can coordinate two moles of formic acid to promote the reaction with respect to one mole of monoamine functionalized ionic liquids, could only coordinate with one mole of formic acid. Tertiary groups also acted as the base to shift the chemical equilibrium in the hydrogenation. Thus, increasing the number of amino groups in the ionic liquid can enhance the yield of formic acid.

Except, [DAMI][$CF_3CF_2CF_2CF_2SO_3$] ionic liquid, [DAMI][TfO] ionic liquid also gave the appreciable result and we recovered a good amount of formic acid.

After getting delightful results with [DAMI][$CF_3CF_2CF_2CF_2SO_3$] ionic liquid immobilized Ru/Ti-6 with water,

we shifted our study to the catalyst recycling study (Fig. 4). After the reaction, formic acid was isolated with the aid of N_2 gas and the [DAMI][$CF_3CF_2CF_2CF_2SO_3$] ionic liquid immobilized Ru/Ti-6 went for a recycling test after washing with diethyl ether and catalysts pretreatment process. [DAMI][$CF_3CF_2CF_2CF_2SO_3$] ionic liquid immobilized Ru/Ti-6 were recycled up to 8 times with slight loss of their catalytic activity mainly due to the agglomeration of monometallic Ru particles and it was also confirmed by TEM analysis of Ru/Ti-6 (Fig. 4). Significant increase, in the particle size of monometallic Ru particles from 6.82 ($\pm$0.5) nm to 21.0 ($\pm$0.5) nm (due to the agglomeration of monometallic Ru particles) may cause a drop in the catalytic activity of Ru/Ti-6 during recyclability test.

7 Conclusion

We easily synthesized a series of active monometallic Ru/Ti-x catalyst by varying several parameters in order to understand the influence of the preparation method, chemical nature of Ru metal precursors, textural as well as structural properties of titania support. Among all the combinations in impregnation method with TiO_2 (P-25) support, the metallic dispersion depends on the nature of the precursors salt, $RuCl_3 \cdot 3H_2O$ salt inducing the smallest average Ru particle size. The TiO_2 (DT51) gave a very different result depending on the preparation method. The hydrogenation reaction also highlighted that the small particle size of Ru metal has more interaction with reactants and offered good quantity of formic acid. A series of functionalized ionic liquids were screened in order to obtain the good solubility of CO_2 gas as well as to absorb formic acid produced during the hydrogenation reaction. Among, all the tested ionic liquids, [DAMI][$CF_3CF_2CF_2CF_2SO_3$] ionic liquid was found as a promising reaction medium to accommodate CO_2 gas in higher concentration as the cationic and anionic part of this ionic liquid equipped with good CO_2-phillic combination. It was clearly observed from our experimental results that one mole of diamine-functionalized ionic liquids, can coordinate with two mole of formic acid to promote the reaction other than mono amine functionalized ionic liquid.

As per above promising development in terms of catalyst and reaction medium, we obtained the formic acid with highest TON value with Ru/Ti-6 in [DAMI][$CF_3CF_2CF_2CF_2SO_3$] ionic liquid medium. Effect of water was also studied during the CO_2 hydrogenation reaction. Eight times catalyst recycling, low catalyst loading and ligand free approach were the some other important outcomes of this proposed protocol.

References

1. Pan M, Brush AJ, Pozun ZD, Ham HC, Yu W-Y, Henkelman G, Hwanga GS, Mullins CB (2013) Chem Soc Rev 42:5002–5013
2. Nerozzi F (2012) Platin Metal Rev 56:236
3. Irfan M, Glasnov TN, Kappe CO (2011) ChemSusChem 4:300
4. Schmidt O (1933) Chem Rev 12:363
5. Navalikhina MD, Krylov OV (1998) Heterogeneous hydrogenation catalysts. Russ Chem Rev 67:587
6. Pinna F (1998) Catal Today 41:129
7. Clapham B, Reger TS, Janda KM (2001) Tetrahedron 57:4637
8. Brunel D, Blanc AC, Galarneau A, Fajula F (2002) Catal Today 73:139
9. Taguchi A, Schüth F (2005) Microporous Mesoporous Mater 77:1
10. Ono Y (2003) J Catal 216:406
11. Rao CNR, Kulkarni GU, Thomasa PJ, Edwardsb PP (2000) Chem Soc Rev 29:27
12. Mody VV, Siwale R, Singh A, Mody HR (2010) J Pharm Bioallied Sci 2:282
13. Campelo JM, Luna D, Luque R, Marinas JM, Romero AA (2009) ChemSusChem 2:18
14. Zahmakıran M, Ozkar S (2011) Nanoscale 1:3462
15. Cuenya BR (2010) Thin Solid Films 518:3127
16. Costaa NJS, Rossi LM (2012) Nanoscale 4:5826
17. Campelo JM, Luna D, Luque R, Marinas JM, Romero AA (2009) ChemSusChem 2:18
18. Kim BH, Hackett MJ, Park J, Hyeon T (2014) Chem Mater 26:59
19. Micheli L (1984) Am Cream Soc Bull 54:694
20. Siefering KL, Griffin GL (1990) J Nanosci Nantechnol 14:3137
21. Kumar VP, Harikrishna Y, Nagaraju N, Chary KVR (2014) Indian J Chem 53A:516
22. Zhao J, Ma L, Xu L-X, Feng F, Li X-N (2014) Chin Chem Lett 25:1137
23. Bagheri S, Julkapli N, Bee Abd Hamid HS (2014) Sci World J 2014:1
24. Ratti R (2014) Adv Chem 2014:1
25. Santos E, Albob J, Irabien A (2014) RSC Adv 4:40008
26. Scholten JD, Leal BC, Dupont J (2012) ACS Catal 2:184
27. Sánchez LMG, Meindersma GW, Haan ABD (2007) Chem Eng Res Des 85:31
28. Sánchez LMG, Meindersma GW, Haan ABD (2011) Chem Eng J 166:1104
29. Rahmana MH, Siajb M, Larachi F (2010) Chem Eng Process 49:313
30. Calleja ET, Skinner J, Tauste DG (2013) J Chem 2013:1
31. Srivastava V (2014) Catal Lett 144:1745
32. Srivastava V (2014) Catal Lett 144:2221
33. Zhang Z, Xie Y, Li W, Hu S, Song J, Jiang J, Han B (2007) Angew Chem Int Ed 47:1127
34. Yang Z-Z, He L-N (2014) Beilstein J Org Chem 10:1959
35. Abidoyea LK, Khudaidaa KJ, Das DB (2015) Crit Rev Environ Sci Technol 45:1105
36. Huff CA, Sanford MS (2011) J Am Chem Soc 133:18122
37. Saeidia S, Amina NAS, Rahimpourb MR (2014) J CO2 Util 5:66
38. Fechete I, Vedrine JC (2015) Molecules 20:5638
39. Ravanchi MT, Sahebdelfar S (2015) Appl Petrochem Res 4:63